ISSN 0252-1075
Contribution from IITM
Research Report No. RR-142
ESSO/IITM/MM/SR/04(2018)/193

The 10-20 day intraseasonal variation of the South Asian summer monsoon simulated by GFDL models in the AMIP experiment of CMIP5

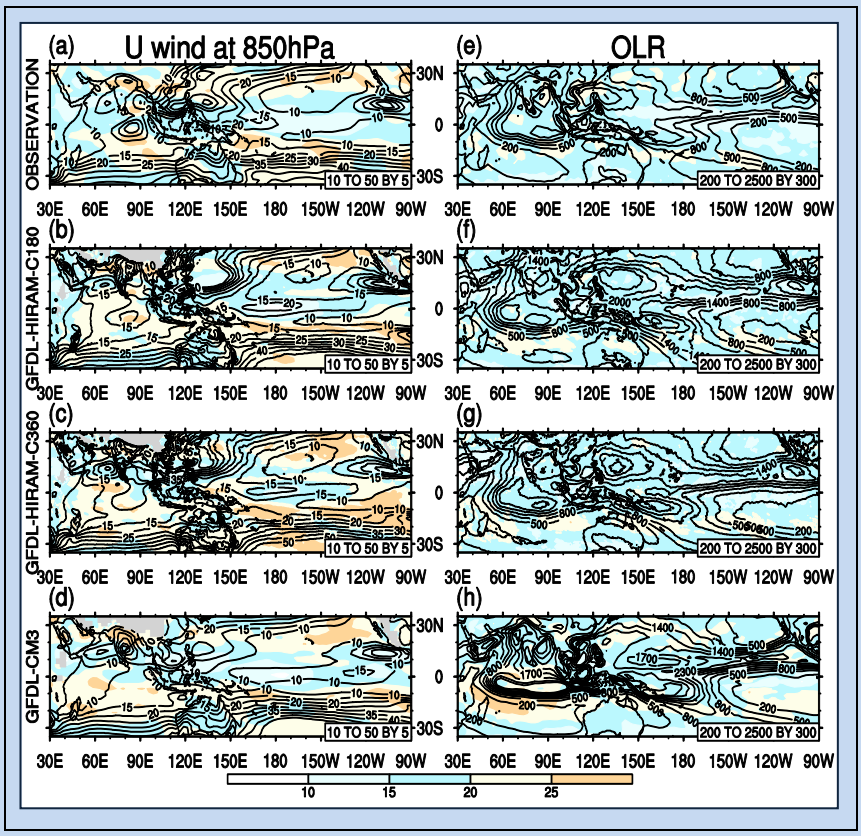

Sujata K. Mandke, Prasanth A. Pillai and A.K. Sahai

Indian Institute of Tropical Meteorology (IITM)
Earth System Science Organization (ESSO)
Ministry of Earth Sciences (MoES)
PUNE, INDIA
http://www.tropmet.res.in/

ISSN 0252-1075
Contribution from IITM
Research Report No. RR-142
ESSO/IITM/MM/SR/04(2018)/193

The 10-20 day intraseasonal variation of the South Asian summer monsoon simulated by GFDL models in the AMIP experiment of CMIP5

Sujata K. Mandke, Prasanth A. Pillai and A. K. Sahai

***Corresponding Author Address:**
Dr. (Smt.) Sujata K. Mandke
Indian Institute of Tropical Meteorology,
Dr. Homi Bhabha Road, Pashan, Pune – 411 008, INDIA
E-mail: amin@tropmet.res.in
Phone: +91-20-25904508

Indian Institute of Tropical Meteorology (IITM)
Earth System Science Organization (ESSO)
Ministry of Earth Sciences (MoES)
PUNE, INDIA
http://www.tropmet.res.in/

DOCUMENT CONTROL SHEET

Earth System Science Organization (ESSO)
Ministry of Earth Sciences (MoES)
Indian Institute of Tropical Meteorology (IITM)

ESSO Document Number
ESSO/IITM/MM/SR/04(2018)/193

Title of the Report
The 10-20 day intraseasonal variation of the South Asian summer monsoon simulated by GFDL models in the AMIP experiment of CMIP5

Authors
Sujata K. Mandke, Prasanth A. Pillai and A. K. Sahai

Type of Document
Scientific Report (Research Report)

Number of pages and figures
28, 06

Number of references
55

Keywords
Intraseasonal oscillation, Asian summer monsoon, CMIP5, AMIP

Security classification
Open

Distribution
Unrestricted

Date of Publication
June 2018

Abstract

The present study investigates intraseasonal variability with focus on 10-20 day period of Intraseasonal Oscillation (ISO) associated with south Asian summer monsoon. Atmosphere-only simulations of three Geophysical Fluid Dynamics Laboratory (GFDL) General Circulation Models (GCMs) from Atmospheric Model Intercomparison Project (AMIP) of Coupled Model Intercomparison Project phase 5 (CMIP5) are used. Results suggests that it remains challenging for atmosphere-only simulations of GFDL GCMs from CMIP5/AMIP to faithfully represent the amplitude and periodicities of two ISO modes namely 30-60 day and 10-20 day, along with propagation characteristics of 10-20 day mode, despite higher horizontal resolution .

Summary

During boreal summer season, intraseasonal variability of south Asian monsoon is manifestation of a superposition of 10-20 day and 30-60 day intraseasonal oscillations and is considered as the primary building block of south Asian summer monsoon. The quasi-periodic variability of boreal summer intraseasonal oscillation determines the strength of the seasonal mean monsoon. Due to profound consequences of south Asian summer monsoon rainfall variability on economy and society, it is essential to understand the complex space–time characteristics of the intraseasonal variability, its simulation and prediction. In contrast to the extensive research devoted toward understanding the genesis, scale-selection and spatial structure of 30-60 day oscillation of south Asian summer monsoon, very few studies have addressed these features of 10-20 day mode. Therefore, in the present study, key aspects of 10-20 day mode of intraseasonal oscillation has been examined using atmosphere-only simulations of three Geophysical Fluid Dynamics Laboratory (GFDL) General Circulation Models (GCMs) from Atmospheric Model Intercomparison Project (AMIP) of Coupled Model Intercomparison Project phase 5 (CMIP5). Two of the GCMs are GFDL high resolution atmospheric models at different horizontal resolution and third "GFDL-CM3" model is of moderate resolution with updated atmospheric model component. There are substantial deficiencies in the simulation of intraseasonal variability of south Asian summer monsoon, in particular no model is able to capture the pronounced spectral peak corresponding to 30-60 day period and the periodicity of simulated oscillation tended to be too short (< 30 days). Intraseasonal oscillation with 10-20 day period is associated with westward propagation from the western tropical Pacific to Arabian sea along the monsoon trough. Only "GFDL-CM3" model simulated westward propagation of 10-20 day mode in low-level zonal wind, though the extent is less than observed. In conclusion, the ability of three GFDL GCMs from CMIP5/AMIP to simulate intraseasonal variability of south Asian summer monsoon has remained problematic, irrespective of high horizontal resolution and updated atmospheric model component.

Contents

The 10-20 day intraseasonal variation of the South Asian summer monsoon simulated by GFDL models in the AMIP experiment of CMIP5

Sujata K. Mandke, Prasanth A. Pillai and A. K. Sahai

Indian Institute of Tropical Meteorology, Pune, India

Abstract

The ability of three Geophysical Fluid Dynamics Laboratory (GFDL) General Circulation Models (GCMs) to simulate the intraseasonal variability with focus on 10-20 day period of Intra-seasonal Oscillation (ISO) associated with South Asian Summer Monsoon has been studied as part of the Atmospheric Model Intercomparison Project (AMIP) of Coupled Model Intercomparison Project phase 5 (CMIP5). Atmosphere-only simulations of three GFDL GCMs prescribed with observational sea surface temperature (SST) and sea ice as forcing during the period 1979-2008, were evaluated by comparing with observations. Two of the GCMs are GFDL global High Resolution Atmospheric Model (HiRAM) and third "GFDL-CM3" model is of moderate resolution. The two HiRAMs namely "GFDL-HIRAM-C180" and "GFDL-HIRAM-C360" are same but have different horizontal resolutions. "GFDL-CM3" model has updated version of atmospheric component compared to HiRAMs.

During boreal summer season (June-September), all three GCMs capture broad features of observed distribution of mean precipitation and zonal wind at 850hPa (U850) reasonably well. However, there are several notable differences between GCMs and observation in regard to details of mean precipitation such as location and strength of Intertropical Convergence Zone, precipitation peak over south east equatorial Indian ocean and Bay of Bengal. Low-level westerlies over Asian region extends too far eastward in two HiRAMs. Onset of monsoon in GCMs matches observed onset except it is late in "GFDL-HIRAM-C180" model. Peak precipitation during summer monsoon season over central Indian region is overestimated by "GFDL-CM3" model. Power spectrum analysis of summer season outgoing longwave radiation (OLR) averaged over extended India, equatorial Indian ocean and Bay of Bengal revealed that none of the GCMs has captured the dominance of 30-60 day mode of ISO, except "GFD-HIRAM-C180" over equatorial Indian ocean. In general, over all four key domains, there is a tendency for GCMs to simulate shorter period (< 30 days) of ISO than in the observation.

Variance of summer season unfiltered U850 in two HiRAMs compare well with observation, except differ over Indian land region and Arabian sea. All three GCMs captured variance of 10-20 day filtered U850, but for slight overestimation over Indian ocean. Similarly, variance of unfiltered and 10-20 day filtered OLR in two HiRAMs resemble observation. "GFDL-CM3" overestimates both unfiltered and 10-20 day filtered OLR variance, particularly overestimates intraseasonal variance over Indian ocean. Westward propagation of 10-20 day mode of ISO in observed U850 is evident from west Pacific to Indian summer monsoon region. "GFDL-CM3" model displayed coherent westward propagation in U850 but the extent is less as compared to observation. Both HiRAMs failed to capture westward propagation of 10-20 day mode of ISO in U850. Results of the study suggests that it remains challenging for atmosphere-only simulations of GFDL GCMs at higher horizontal resolution to faithfully represent two modes of ISO namely 30-60 day and 10-20 day including their amplitude, periodicities and propagation characteristics.

1. Introduction

The tropical atmosphere exhibits intraseasonal variability (ISV) in the form of intraseasonal oscillations (ISO), on time scales between weather and climate. The ISV in the tropics is of considerably larger magnitude and plays an extremely important role in the nature and evolution of the Asian summer monsoon (ASM) (Waliser, 2006). During summer monsoon season, ISV of ASM is dominated by quasi-periodic ISO (referred here as Boreal Summer Intraseasonal oscillations; BSISO) in the form of wet (active) spells of above-normal rainfall, separated by dry (break) spells of below-normal rainfall (Goswami, 2005; Rajeevan et al., 2010), on time scales longer than 10 days but shorter than a season. These active/break phases of South ASM are manifestations of the superposition of westward propagating high frequency 10-20 day mode (Krisnamurthy and Bhalme, 1976; Krishnamurthi and Ardunay, 1980; Chen and Chen, 1993) and northward propagating low frequency 30-60 day mode (Yasunari, 1979, 1980, 1981; Sikka and Gadgil, 1980, Lau and Chan, 1986; Mehta and Krishnamurthy, 1988, Gadgil, 1990, Wang and Rui, 1990; Annamalai and Sperber, 2005 among others). ISV generated by ISO, is highly complex inherent mode of variability within the ASM system, one that govern its active and break periods (Gadgil and Asha, 1992, Gadgil, 2003, Webster et al., 1998; Annamalai and Slingo, 2001), modulates the embedded synoptic variability (Goswami et al., 2003) and significantly influence the seasonal mean and its interannual variability (Krishnamurthy and Shukla, 2000; Goswami and Ajayamohan, 2001). The amplitude of ISV of ASM rainfall is much larger than that of the interannual variability of seasonal mean (Goswami, 2005). Consequently this ISV is extremely important for rainfall predictions and their socio-economic applications. Comprehensive review on all facets of ISV of ASM region is available (Goswami, 2005; Wailser, 2006 and references therein).

Simulating the space-time features of the BSISO is still difficult test for most General Circulation Models (GCMs), not only for initial atmospheric GCMs (AGCM) (Gadgil and Sajani, 1998; Rajendran et al., 2002; Waliser et al., 2003; Klingaman et al., 2008 among others), but also for the latter atmosphere-ocean coupled GCMs (CGCM) (Kemball-Cook et al., 2002; Fu et al. 2003; Fu and Wang 2004; Zheng et al. 2004; Rajendran and Kitoh, 2006; Mandke et al., 2013; Sur et al., 2013, among others), to the recent state-of-the-art CGCMs intercomparisons (Lin et al., 2008; Sperber and Annamalai, 2008; Xavier et al., 2008; Sabeerali et al., 2013 among others). Recently, number of international research groups carried out a set of climate runs for the Coupled Model Intercomparison Project phase 5

(CMIP5). These GCMs runs has been conducted for the Intergovernmental Panel on Climate Change (IPCC) Fifth Assessment Report (AR5) (Taylor et al., 2012). Some CMIP5 modelling groups performed experiments with different resolutions and some also made Atmospheric Model Intercomparison Project (AMIP) simulations, in addition to the standard coupled runs. Possible causes for the difficulties in BSISO simulation by GCMs cannot be understood, as there are several differences in the model treatments among GCMs. Experiments are therefore needed to examine the effect of different treatments for the same physical or dynamical processes using a single model. This prompted us to consider single model from National Oceanic and Atmospheric Administration (NOAA) Geophysical Fluid Dynamics Laboratory (GFDL), which is able to simulate modest Indian summer monsoon climatology (Mandke et al., 2007) and relatively robust BSISO (Waliser et al., 2003; Lin et al., 2008; Sabeerali et al., 2013). Simulations of the same model at diverse horizontal resolution comprising of ultra-high, high and medium resolution are available only for GFDL and MRI models in CMIP5 AMIP. We have selected GFDL model in the present study as our aim is to study the dependence of intraseasonal activity on model's horizontal resolution. A worthwhile extension of this study will be to examine ISV simulations of MRI model at diverse resolution. Recent intercomparisons (Lin et al., 2008; Sabeerali et al., 2013) have shown that the current state-of-the-art CGCMs also have difficulties in representing the BSISO over ASM. Thus, we have selected atmosphere-only simulations of three versions of GFDL GCMs from CMIP5 AMIP experiment. While considerable attention has been paid to address 30-60 day mode of ISO, not many studies address the 10-20 day ISO mode. So our emphasize is on 10-20 day mode of ISO.

In view of the above scientific background, in the present study, we attempt to examine the ISV of ASM with emphasis on 10-20 day mode of ISO in three GFDL GCMs' simulations from CMIP5 AMIP. Two of the GCMs are GFDL global High Resolution Atmospheric Model (HiRAM) have different horizontal resolution while the third model "GFDL-CM3" has relatively lower horizontal resolution compared to HiRAMs and also includes updated version of atmospheric component. The research report is arranged as follows: Details of both model and observed datasets followed by the analysis methods are introduced in section 2. Description of results is given in section 3. Section 4 provides the conclusion.

2. Datasets and methodology

2.1 Model and observed datasets

Simulations from three GFDL GCMs participating in AMIP experiment of CMIP5 are analyzed in the present study. Brief details of the selected GCMs are listed in Table 1, indicating horizontal and vertical resolution. Further information on individual GCMs are available (at http://cmip-pcmdi.llnl.gov/cmip5/; https://www.gfdl.noaa.gov/model-development/). "Time-slice" integrations of present-day climate period (1979-2008) from AMIP are used, in which AGCMs are integrated with observed sea surface temperature (SST) and sea ice as lower-boundary conditions at the oceanic grid points. Brief summary of the CMIP5 experimental design is described by Taylor et al. (2012). HiRAM is based on atmospheric component AM2 (Anderson et al., 2004), with increased horizontal resolution and simplified parameterisations for moist convection and large-scale cloudiness (Zhao et al., 2009; Chen and Lin, 2011; Held and Zhao, 2011). Atmospheric component AM3 of "GFDL-CM3" model is updated version, with improved atmospheric physics and chemistry, which include interactive tropospheric and stratospheric chemistry, chemistry-climate feedbacks, land and ocean carbon cycles and cloud-aerosol interactions (Donner et al., 2011).

Precipitation, Outgoing longwave radiation (OLR) and zonal wind at 850hPa (U850) for 'r1i1p1' ensemble of three GFDL GCMs are used. The ensemble identifier 'r' denote model integration initialized from different times of a control run, letter 'i' distinguish between initialization of models with different methods and letter 'p' for different perturbed physics. The output from these models is stored at GFDL's data portal and is publicly accessible (http://data1.gfdl.noaa.gov/). We have used multiple observed datasets along with reanalysis data for validation of GCMs simulations.

- Global Precipitation Climatology Project (GPCP) 1^0 long x1^0 lat resolution precipitation data (Adler et al., 2003)
- NOAA interpolated daily mean OLR data (Liebmann and Smith, 1996).
- Daily gridded data of U850 from National Centre for Environmental Prediction-National Centre for Atmospheric Research (NCEP–NCAR) reanalysis (Kalnay et al., 1996)

2.2 Methodology

The ability of GCMs to simulate the intraseasonal variation has been studied by identifying dominant periodicities through power spectrum analysis. Times series power spectra is estimated using Fast Fourier Transforms method. Power spectrum is calculated from seasonally stratified OLR based on 122 days seasonal period from 1st June-30th September. Unfiltered anomaly data are averaged over region and the spectra are calculated separately for each year. From each segment, time mean is removed. The spectra are then averaged across all years for the given season. The ISO calculation is based on 10-20 day band pass filtered (Duchon, 1979) daily anomaly of precipitation, OLR and U850.

3. Results

3.1 Seasonal mean monsoon

Better representation of ISO in a GCM is intimately related to the ability of the GCM to simulate seasonal mean climate (Slingo et al., 1996; Gadgil and Sajani, 1998; Waliser et al., 2003; Ajayamohan and Goswami, 2007). Therefore, analysis of a number of relevant mean fields is an important beginning for assessment of BSISO simulations by GCMs. For example, characteristics of convective mean state that are relevant to BSISO include latitudinal and zonal locations of the Intertropical Convergence Zone (ITCZ), and a realistic simulation of lower tropospheric westerly winds, especially their zonal extent across the warm pool of the Indian and Pacific oceans. Mean fields such as precipitation and U850 for boreal summer season from June-September are presented in Figure 1. Comparison of mean precipitation from GPCP observation and three GCMs is illustrated in Figure 1(a-d) respectively. Similarly, figure 1(e-h) shows mean U850 from NCEP reanalysis observation and three GCMs respectively. An essential condition for simulation of BSISO in GCMs is to realistically simulate the summer-mean climatology of precipitation, especially the three main precipitation centers located over equatorial central-eastern Indian ocean, Bay of Bengal, and the tropical west Pacific (Sperber and Annamalai, 2008). Precipitation maxima over equatorial central-eastern Indian ocean is overestimated and extend westward in all three GCMs, which is surplus in “GFDL-CM3” model (Figure 1d). Location and intensity of Bay of Bengal centre varies among all three GCMs and also differ from observation. There are several notable differences between GCMs and observation in regard to details such as location and strength of ITCZ over Pacific ocean. Most significant bias in three GFDL GCMs

simulations is the location and intensity of ITCZ over Pacific ocean. Both HiRAMs tend to simulate two zonal bands of precipitation in the central Pacific ocean. ITCZ over central Pacific ocean in "GFDL-CM3" model is shifted farther southward as compared to observation. There is excess precipitation over central Indian region and rain shadow region over south-east peninsular India is narrower in "GFDL-CM3" model than observed. All three GCMs exhibit divergence in capturing the intensity, location and spatial extent of small precipitation maxima over west coast of India.

In the northern hemisphere, westerly winds are noticed in observed mean U850, especially their zonal extent across the warm pool of Indian and west Pacific oceans, while easterlies are observed in the southern hemisphere (Figure 1e). In both HiRAMs, in northern hemisphere westerlies extends too far eastward (Figure 1(f-g)), more stronger and farther in "GFDL-HIRAM-C180", leading to eastward extension of ITCZ and thus larger precipitation over this extended region of westerlies (Figure 1(b-c)) than observed (Figure 1a). On the contrary, zonal extent of westerlies in "GFDL-CM3" is less (Figure 1h) compared to that in observation (Figure 1e). In addition, northward extent of westerlies over India in both HiRAMs (Figure 1(f-g)) is in good agreement with observation (Figure 1e), while in "GFDL-CM3" model (Figure 1h), it is relatively southward. Strength and extent of southern hemisphere easterlies are simulated realistically by all three GCMs.

3.2 Annual cycle of precipitation

The Annual cycle of precipitation averaged over an area (65^0E-88^0E, 18^0N-28^0N) over Indian region is delineated for three GCMs and corresponding GPCP observation in Figure 2. This region is selected because significant rainfall fluctuations between active and break spells occur over this region (Rajeevan et al., 2010). Monsoon onset in "GFDL-HIRAM-C360" and "GFDL-CM3" models matches with observation while onset is late in "GFDL-HIRAM-C180". Precipitation exceeds observation from mid-June till December and maxima during summer monsoon is much larger in "GFDL-CM3" model. It is evident from figure 2 that "GFDL-HIRAM-C180" overestimated precipitation in the post monsoon season.

3.3 Power spectrum analysis

Power spectrum averaged over four key domains (described in Table 2) is computed, to reveal GCMs capability to produce ISV. Power spectrum of OLR from NOAA observation and three GCMs averaged over extended India (EIND) is illustrated in Figure 3(a-d) and over Indian ocean (IO) in Figure 3(e-h) respectively. Similarly, power spectrum from observation and three GCMs over other two domains namely Bay of Bengal (BB) and West Pacific (WPAC) are shown in Figure 4(a-d) and Figure 4(e-h) respectively. The null, 5% and 95% red noise significance levels are included for the power spectra delineated in both figures 3(a-h) and figure 4(a-h).

Power spectrum of observed OLR over EIND clearly shows two prominent peaks significant at 95%, one in low-frequency mode of 30-60 day and other in relatively higher frequency band (20-30 day), separated from synoptic variability (<10 days). All three GCMs fail to produce 30-60 day peak over EIND. Both HiRAMs simulated only high frequency synoptic scale (period < 10 day), while "GFDL-CM3" model captured peak corresponding to 20-30 day scale in addition to synoptic scale (<10 day) over EIND. All GCMs also exhibit spurious large power (which is not significant at 95%) in low-frequency band of period greater than 100 days over EIND. Spectra of observed OLR over IO display peak corresponding to 30-60 day period with significant power separated from quasi-biweekly (10-20 day) and synoptic scale. "GFDL-HIRAM-C180" is able to represent all these period bands over IO, though power is considerably less than observed. Inability of "GFDL-HIRAM-C360" and "GFDL-CM3" in simulating 30-60 day period over IO is clear from figure 3(g-h), while they successfully simulated quasi-biweekly and synoptic scale over this region.

Spectral peaks at 30-60 day, 10-20 day and less than 10 days significant at 95% are evident in the observed spectra over BB. With the exception of low-frequency 30-60 day peak, other spectral peaks over BB are well simulated by all three GCMs. Observation suggests dominance of significant power for periods less than 30 days over WPAC, which are credibly captured by all three GCMs.

GCMs failed to capture observed low frequency mode (period > 30 days) of ISV over all four domains, except for "GFDL-HIRAM-C180" over IO. On the contrary, all three GCMs simulate significant power in relatively higher frequency band (period < 30 days). This implies that GFDL models mean rain has a considerable contribution from the high frequency events.

3.4 Variance patterns of 10-20 day mode of ISO

In preceding sections climatological features and ISV of ASM were assessed. In this subsection, performance of GCMs in simulating unfiltered daily as well as intraseasonal variance of 10-20 day mode of ISO in U850 and OLR is examined. Spatial structure of variance of unfiltered U850 (contours) during summer season (June-September) for NCEP observation and three GCMs are depicted in Figure 5(a-d) respectively. In the same figure 5(a-d), prominence of 10-20 day mode of ISO is emphasized by shading the percent variance accounted by the 10-20 day band relative to unfiltered variance. Identical illustration of unfiltered variance (contour) and intraseasonal 10-20 day mode variance (shade) of OLR for NOAA observation and three GCMs is shown in figure 5(e-h) respectively. Comparative performance of unfiltered U850 variance between GCMs and observation shows that over Pacific ocean all GCMs resemble observation, while over Indian land region GCMs differs from observation. Over Indian ocean "GFD-HIRAM-C180" matches with observation, while other two GCMs disagree. Observation (Figure 5a) shows three centres of maxima of 10-20 day variance of U850 over northern India, central equatorial Indian ocean and south BB. "GFDL-HIRAM-C180" (Figure 5b) captured these three maxima well, while other two GCMs (Figure 5 (c-d)) failed. "GFDL-CM3" model (Figure 5d) tends to overestimate 10-20 day variance of U850 over northern India.

Variance of (unfiltered) OLR is larger in three GCMs (Figure 5(f-h)), excessively large in "GFDL-CM3" model than corresponding observation (Figure 5e). Intraseasonal (10-20 day) variance of observed OLR varies between 15-20% over majority of region with 20-25% over some very small regions. Both HiRAMs realistically simulated this intraseasonal variance and "GFDL-CM3" model overestimated over equatorial and southern Indian ocean.

3.5 Propagation features of 10-20 day mode of ISO

Within a particular monsoon season, 10-20 day mode of ISO is characterised by westward propagating intraseasonal anomalies from western pacific to Indian region (Krishnamurti and Ardunay, 1980; Chen and Chen, 1993; Annamalai and Slingo, 2001; Chatterjee and Goswami, 2004). In this subsection, ability of GCMs to simulate this fundamental propagating and time varying nature of 10-20 day mode of ISO during ASM is considered. The meridional and zonal propagation of ISO computed using lag regression analysis are compared among the three GFDL GCMs and corresponding observation. For this

purpose, 10-20 day filtered precipitation and U850 anomalies at each grid point are regressed at the different time lags with respect to a reference time series created by area-averaging the 10-20 day filtered precipitation anomalies over the south Bay of Bengal region (80^0E-90^0E, 5^0N-10^0N). Hovmöller diagram of regressed 10-20 day filtered precipitation and U850 anomalies are described to diagnose propagation characteristics of 10-20 day mode of ISO during boreal summer season. GPCP precipitation and U850 from NCEP-NCAR reanalysis data is used for observation.

Lag-longitude illustration of regressed 10-20 day filtered precipitation anomalies (shade) overlapped with U850 anomalies (contour) averaged between 5^0N and 15^0N is shown from day -25 to +25 days, for observation and three GCMs in figure 6(a-d) respectively. U850 observation (Figure 6a) indicate westward propagation from western Pacific ocean into the Indian summer monsoon region. Westward propagation is not noticed in observed precipitation. "GFDL-CM3" model displayed coherent westward propagation in U850 but the extent is less compared to observation. Both HiRAMs failed to capture westward propagation in U850, which is a basic feature of 10-20 day mode of ISO. Like lag-longitude, lag-latitude plot of regressed 10-20 day filtered precipitation (shade) anomalies overlapped with U850 anomalies (contour) averaged over longitude 80^0E-100^0E is delineated for observation and three GCMs in figure 6(e-h) respectively. 10-20 day mode of ISO is associated with northward propagation of precipitation from equator to 20^0N from lag 20 days to lag 0 in observation (figure 6e). "GFDL-HIRAM-C180" and "GFDL-CM3" model (figures 6f and 6h) exhibit northward propagation, which is much slow as compared to corresponding observation.

4. Conclusions

Seasonal variability of ASM rainfall depends on the spatio-temporal evolution of the ISO. Summer monsoon rainfall associated with the ISO has profound impact on the socio-economic growth in the Asian monsoon region. Therefore, much of the focus of attention in recent years has been on understanding the complex space–time characteristics of the ISO, its realistic simulation and prediction. Keeping this in view, in the present study, we presented the results of the assessment of the ISV of ASM in atmosphere-only simulations of three GFDL GCMs. Among three GCMs considered, two are GFDL HiRAMs at different horizontal resolution. Third "GFDL-CM3" model is of moderate resolution (refer table 1 for details of GCMs resolution) with updated atmospheric model component. The present day climate period (1979-2008) from CMIP5 AMIP are analysed.

The power spectrum analysis for four key regions (provided in table 2) and maps of intraseasonal (10-20 day) variance are examined to assess the robustness of GCM simulated ISV. Three GFDL GCMs tend to simulate higher-frequency (10-20 day) mode of ISO but unable to capture observed low-frequency (30-60 day) mode over EIND, IO and BB, with exception of "HiRAM-C180" over IO. All three GFDL GCMs are able to simulate structure of 10-20 day filtered variance of U850, except slight overestimation over Indian ocean. Two HiRAMs simulated the spatial pattern of intraseasonal (10-20 day) variance of OLR while "GFDL-CM3" largely overestimated, particularly over Indian ocean. We demonstrated from the analysis that "GFDL-CM3" model simulated westward propagation, a major characteristic of the 10-20 day mode of ISO. In conclusion, results suggest that atmosphere-only simulations of three GFDL GCMs in CMIP5 AMIP have difficulties in simulating ISV of ASM, irrespective of high horizontal resolution and updated atmospheric model component. With the exception of "GFDL-CM3" model, simulation of westward propagation of the 10-20 day mode of ISO is also problematic in GCMs. This implies the significance of suitable physics schemes to be used in high-resolution models for achieving realistic ISV simulation. Hence, it is meaningful to examine the role of model resolution in the presence of suitable physics schemes particularly convection (Slingo et al., 1996) on simulation of ISV.

There is now convincing evidence from both observations (Bhat et al., 2001; Sengupta and Ravichandran, 2001; Sengupta et al., 2001; Vecchi and Harrison, 2002) and modeling studies (Fu and Wang, 2004; Zheng et al., 2004) that ISO involves coupling with the ocean, which may therefore require an interactive ocean system for its reasonable simulation. Studies have also emphasized that realistic air-sea coupling is fundamental in defining characteristics and maintaining the observed space-time features of ISO (Fu et al., 2003; Fu and Wang, 2004; Rajendran and Kitoh 2006; Sur et al., 2013; Mandke et al., 2013 among others). Air-sea coupling plays a critical role in organisation and intensification of ISO (Kemball-Cook et al., 2002). Despite the biases in three GCMs, one of the potential explanation for the poor performance in the representation of ISV in the atmosphere-only simulations of GFDL GCMs in the present study is the absence of air-sea interaction. Coupled GCMs therefore provide a more promising tools and presents prospects for future research to explore role of air-sea interaction in the simulation of the ISV and 10-20 day mode of ISO. This research problem will be addressed in the future work.

Acknowledgements

We thank Director, Indian Institute of Tropical Meteorology (IITM), Pune for all the support to carry out this work. IITM is funded by the Ministry of Earth Sciences, Government of India, New Delhi. We thank reviewers Dr. Samir Pokhrel and Dr. Hemant Chaudhari, scientist, IITM, Pune for extremely careful review and constructive comments which helped a lot in improving the research report. Especially the quality of figures is greatly enhanced in the revised version.

We acknowledge the World Climate Research Programme's Working Group on Coupled Modelling, which is responsible for Coupled Model Intercomparison Project (CMIP). For CMIP, the U.S. Department of Energy's Program for Climate Model Diagnosis and Intercomparison provides coordinating support and led development of software infrastructure in partnership with the Global Organization for Earth System Science Portals. Authors would like to acknowledge Geophysical Fluid Dynamics Laboratory modelling group for producing and making available their model simulations (http://data1.gfdl.noaa.gov/). Authors are thankful to National Center for Environmental Prediction (NCEP) for the reanalysis data sets (http://www.esrl.noaa.gov/psd/) used here. Authors acknowledge Global Precipitation Climatology Project (GPCP) rainfall dataset (http://precip.gsfc.nasa.gov/). All data sources used in the report are dully acknowledged. Majority of analysis and some figures are made using National Center for Atmospheric Research (NCAR) Command Language (NCL) (Version 6.4.0) [Software]. (2017) Boulder, Colorado: UCAR/NCAR/CISL/VETS. http://dx.doi.org/10.5065/D6WD3XH5. Authors thank the NCL development team in particular, Prof. Dennis Shea and Mary Haley for all the assistance provided. We also gratefully acknowledge Brian Doty from Center for Ocean Land Atmosphere, U.S.A., for Grid Analysis and Display System (GrADS) tool, which has been used to draw some of the figures.

Table 1. Details of three GFDL models that participated in CMIP5/AMIP and are used in the present study

S. No.	Model	Horizontal resolution longitude x latitude	Number of vertical levels
1.	GFDL-CM3	2.5^0 x 2^0	48
2.	GFDL-HIRAM-C180	0.625^0 x 0.5^0	32
3.	GFDL-HIRAM-C360	0.3125^0 x 0.25^0	32

Table 2. Domains for power spectrum analyses

Extended India (EIND)	Indian ocean (IO)	Bay of Bengal (BB)	West Pacific (WPAC)
10^0N-28^0N, 65^0E-88^0E	10^0S-5^0N, 75^0E-100^0E	10^0N-20^0N, 80^0E-100^0E	10^0N-25^0N, 115^0E-140^0E

References

Adler RF, Huffman GJ, Chang A, Ferraro R, Xie P, Janowiak J, Rudolf B, Schneider U, Curtis S, Bolvin D, Gruber, A, Susskind J, Arkin P, and Nelkin E (2003) The version-2 global precipitation climatology project (GPCP) monthly precipitation analysis (1979-present). *J Hydrometeorol,* 4:1147-1167.

Ajayamohan, R.S. and Goswami, B.N., 2007, Dependence of simulation of boreal summer tropical intraseasonal oscillations on the simulation of seasonal mean, *J. Atmos. Sci.*, 64, 460–478, doi:10.1175/JAS3844.1.

Anderson J., Balaji, V., Broccoli, A.J. et al., 2004, The new GFDL global atmosphere and land modelAM2/LM2:Evaluation with prescribed SST simulations, *J. Climate*, 17, 4641–4673.

Annamalai, H. and J.M. Slingo, 2001, Active/break cycles: diagnosis of the intraseasonal variability of the Asian Summer Monsoon, *Climate Dynamics,* 18, 1-2, 85-102.

Annamalai, H. and Sperber, K.R., 2005, Regional heat sources and the active and break phases of boreal summer intraseasonal (30 –50 day) variability, *J. Atmos. Sci.*, 62, 8, 2726–2748.

Bhat, G.S., Gadgil, S., Hareesh Kumar, P.U., Kalsee, S.R., Madhusoodanan, P., Muriz,V .S.N., Prasada Rao, C.U.K., Ramosh Babu, V., Rao, U.G., Rao, R.R. et al., 2001, BOBMEX: The bay of Bengal Monsoon experiment, *Bull. Amer. Met.Soc.*, 82, 10, 2217-2243.

Chatterjee, P. and Goswami, B.N., 2004, Structure, genesis and scale selection of the tropical quasi -biweekly mode, *Q. J. R. Meteorol. Soc.*, 130, 1171–1194.

Chen T.C. and Chen J.M., 1993, The 10-20 day mode of the 1979 Indian monsoon: its relation with the time variation of monsoon rainfall, *Mon Weather Rev,* 121, 2465-2482.

Chen, J-H and Lin, S-J, 2011, The remarkable predictability of interannual variability of Atlantic hurricanes during the past decade, *Geo. Res. Let.,* 138,11, DOI:10.1029/2011GL047629

Donner, Leo J., Bruce Wyman, Richard S Hemler, Larry W Horowitz, Yi Ming, Ming Zhao, J-C Golaz, et al., 2011, The dynamical core, physical parameterizations, and basic simulation characteristics of the atmospheric component AM3 of the GFDL Global Coupled Model CM3, *Journal of Climate*, 24,13, 3484-3519, DOI:10.1175/2011JCLI3955.1 .

Duchon C.E., 1979, Lanczos filtering in one and two dimensions, *J Appl Meteorol*, 18, 1016–1022.

Fu, X. and Wang, B., 2004, The boreal-summer intraseasonal oscillations simulated in a hybrid coupled atmosphere ocean model, *Mon. Wea. Rev.,* 132, 11, 2628-2649.

Fu, X., Wang, B., Li, T. and McCreary, J. P., 2003, Coupling between northward-propagating,

intraseasonal oscillations and sea surface temperature in the Indian Ocean, *J. Atmos. Sci.*, 60, 15,1733–1753.

Gadgil S., 1990, Poleward propagation of the ITCZ: observations and theory, *Mausam*, 41: 285-290

Gadgil, S., 2003, The Indian monsoon and its variability, *Annu. Rev. Earth Planet. Sci*., 31, 429–467.

Gadgil S., and Asha G., 1992, Intraseasonal variation of the summer monsoon. I: observational aspects, *J Meteorol Soc Japan,* 70, 1B, 517-527

Gadgil S., Sajani S., 1998, Monsoon precipitation in the AMIP runs, *Clim Dyn*, 14, 9, 659–689

Goswami, B.N. and Ajaya Mohan, R.S., 2001, Intraseasonal oscillations and interannual variability of the Indian summer monsoon, *J. Climate*, 14, 6, 1180–1198.

Goswami BN, Ajayamohan RS, Xavier PK, Sengupta D., 2003., Clustering of synoptic activity by Indian summer monsoon intraseasonal oscillations, *Geophys. Res. Lett.,* 30, 1431, DOI:10.1029/2002GL016734.

Goswami BN, 2005, South Asian Monsoon In Lau WK-M and Waliser DE (ed) Intraseasonal Variability of the Atmosphere-Ocean Climate System. Springer, Berlin Heidelberg, pp 19–61.

Held, I.M. and Zhao, M., 2011, The response of tropical cyclone statistics to an increase in CO_2 with fixed sea surface temperatures, *J. Clim*., 24, 5353–5364.

Kalney, E, Kanamitsu, M, Kistler, R, Collins, W, Deaven, D, Gandin, L, Chelliah, M.M, Ebisuzaki, W, Higgins, W, Janowiak, J, Mo, K.C, Ropelewski, C, Wang, J, Jenne,R and Joseph, D, 1996, The NCEP/NCAR 40-year reanalysis project, *Bull. Amer. Met. Soc.*, 77, 437-472.

Kemball-Cook S, Wang B., Fu, X., 2002, Simulation of the ISO in the ECHAM-4 model: the impact of coupling with an ocean model, *J Atmos Sci.*, 59, 1433–145

Klingaman, N.P., Inness, P.M., Weller, H. and Slingo, J.M., 2008, The importance of high frequency sea-surface temperature variability to the intraseasonal variability of Indian monsoon rainfall, *J. Clim*., 21, 23, 6119-6140.

Krishnamurthy, V. and Shukla, J., 2000, Intraseasonal and interannual variability of rainfall over India, *J. Climate*, 13, 4366–4377.

Krishnamurti, T.N. and Bhalme, H. N., 1976, Oscillations of monsoon system, Part I: Observational aspects, *J. Atmos. Sci.*, 45, 1937–1954.

Krishnamurti, T.N. and Ardunay, P., 1980, The 10 to 20 day westward propagating mode and breaks in the monsoons, *Tellus*, 32, 15–26.

Lau, K-M and Chan P.H., 1986, Aspects of the 40-50 day oscillation during the northern

summer as inferred from outgoing longwave radiation, *Mon Weather Rev*., 114, 7, 1354-1367.

Liebmann, B., Smith C.A., 1996, Description of a complete (interpolated) outgoing long wave radiation dataset, *Bull Am Meteorol Soc.*, 77, 1275–1277

Lin, J-L, Weickmann, K.M., Kiladis, G.N., Mapes, B.E., Schubert, S.D., Suarez, M.J., Bacmeister, J.T., Lee, M-I , 2008, Subseasonal variability associated with Asian summer monsoon simulated by 14 IPCC AR4 coupled GCMs, *J Clim.*, 21, 4541–4567.

Mandke, Sujata K., Sahai, A.K., Shinde, M.A., Joseph, S. and Chattopadhay, R., 2007, Simulated changes in active/break spells during the Indian summer monsoon due to enhanced CO22 concentrations: assessment from selected coupled atmosphere-ocean global climate models, *International J. of climatology*, 27, 837-859.

Mandke, Sujata K., Shinde, M.A., Sahai, A.K., 2013, The importance of coupled sea surface temperatures to the Northward propagation of summer monsoon Intraseasonal Oscillation, *Indian Institute of Tropical Meteorology research report*, RR-129, pp 1-23.

Mehta, V. M. and Krishnamurti, T. N., 1988, Interannual Variability of 30-50 day wave motion, *J. Meteor. Soc. Japan*, 66, 535–548.

Rajendran, K., Nanjundiah, R.S. and Srinivasan, J., 2002, The impact of surface hydrology on the simulation of tropical intraseasonal oscillation in NCAR (CCM2) atmospheric GCM, *J. Meteor. Soc. Japan*, 80, 1357 –1381.

Rajendran, K. and Kitoh, A., 2006, Modulation of tropical intraseasonal oscillations by atmosphere-ocean coupling, *J. Clim.*, 19, 3, 366-391.

Rajeevan, M., Gadgil, S. and Bhate, J., 2010, Active and break spells of the Indian summer monsoon, *J. Earth Sys. Sci.*, 119, 3, 229–248.

Sabeerali, CT,R., Dandi, A., Dhakate, A., Salunke, K., Mahapatra S. and Rao, S., 2013, Simulation of BSISO in the latest CMIP5 coupled GCMs, *J. Of geophysical research, atmosphere*, 2013,118, 4401-4420.

Sengupta, D. and Ravichandran, M., 2001, Oscillations of Bay o Bengal sea surface temperature during the 1998 summer monsoon, *Geophy. Res. Let.*, 28, 10, 2033-2036.

Sengupta, D., Goswami, B.N. and Senan, R., 2001, Coherent intraseasonal oscillations of ocean and atmosphere during the Asian summer Monsoon, *Geophy. Res. Let.*, 28, 21, 4127-4130.

Sikka, D.R., Gadgil, S., 1980, On the maximum cloud zone and the ITCZ over Indian, longitudes during the southwest monsoon, *Mon Weather Rev.,* 108,11,1840–1853.

Slingo J.M., Sperber, K.R., Boyle, J.S., Ceron, J.P., Dix, M., Dugas, B., Ebisuzaki, W., Fyfe, J. et al., 1996, Intraseasonal oscillations in 15 atmospheric general circulation models: results from an AMIP diagnostic subproject, *Clim Dyn*, 12, 325–357

Sperber, K.R. and Annamalai, H., 2008, Coupled model simulations of boreal summer intraseasonal (30–50 day) variability, Part1: Systematic errors and caution on use of metrics, *Climate Dynamics*, 31, 2-3, 345–372.

Sur, Sharmila, Pillai, P.A., Joseph, S., Roxy, M., Krishna, R.P.M., Chattopadhyay, R., Abhilash, S., Sahai, A.K., Goswami, B.N., 2013 Role of ocean-atmosphere interaction on northward propagation of Indian summer monsoon intra-seasonal oscillations (MISO), *Climate Dynamics*, 41, 1651–1669, DOI:10.1007/s00382-013-1854-1,

Taylor, K.E., Stouffer, R.J. and Meehl, G.A., 2012, An overview of CMIP5 and the experiment design, *Bull. Am. Meteorol. Soc.*, 90,4 85–498.

Vecchi, G.A. and Harrison D.E., 2002, Monsoon breaks and subseasonal sea surface temperature variability in the Bay of Bengal, *J. Clim.*, 15, 1485-1493.

Waliser, D.E., 2006, Intraseasonal variability. In: Wang B (ed) *The Asian monsoon*, chap 5. Praxis Springer, Chichester, pp 203–258

Waliser, D.E., Jin, K., Kang, I-S, Stern, W.F., Schubert, S.D., et al., 2003, AGCM simulations of intraseasonal variability associated with the Asian summer monsoon, *Climate Dynamics*, 21,423–446. doi:10.1007/s00382-003-0337-1

Wang, B., Rui, H., 1990, Synoptic climatology of transient tropical intraseasonal convection anomalies: 1975-1985, *Meteorol Atmos Phys*, 44, 43-61

Webster, P. J., Magana, V. O., Palmer, T. N., Shukla, J., Tomas, R. T., Yanai, M. and Yasunari, T., 1998, Monsoons: Processes, predictability and the prospects of prediction, *J. Geophys. Res.*, 103(C7), 14451–14510.

Xavier, P.K., Duvel, J.-P., Doblas-Reyes, 2008, Boreal summer intraseasonal variability in coupled seasonal hindcasts, *J. Climate*, 21, 17, 4477-4497.

Yasunari, T., 1979, Cloudiness fluctuation associated with the northern hemisphere summer monsoon, *J Meteorol Soc Jpn*, 57, 227–242.

Yasunari, T, 1980, A quasi-stationary appearance of 30–40 day period in the cloudiness fluctuation during summer monsoon over India, *J Meteorol Soc Jpn*, 58, 225–229.

Yasunari, T., 1981, Structure of an Indian summer monsoon system with around 40-day period, *J Meteorol Soc Jpn*, 59, 336–354.

Zhao, M., Held, I.M., Lin, S-J and Vecchi, G.A., 2009, Simulations of global hurricane climatology, interannual variability, and response to global warming using a 50km resolution GCM, *journal of Climate*, 22, 24,6653-6678, DOI:10.1175/2009JCLI3049.1.

Zheng, Y., Waliser, D.E., Stern, W. and Jones, C., 2004, The role of coupled sea surface temperatures in the simulation of the tropical intraseasonal oscillation, *J. Clim.*, 17, 21,4109-4134.

List of figures

Figure 1: Seasonal (June-September) mean precipitation (mm day^{-1}) (a) observation (GPCP) (b) GFDL-HIRAM-C180 model (c) GFDL-HIRAM-C360 model (d) GFDL-CM3 model. Similarly for mean zonal wind at 850hPa (m sec^{-1}) (e) observation (NCEP/NCAR reanalysis) (f) GFDL-HIRAM-C180 model (g) GFDL-HIRAM-C360 model (h) GFDL-CM3 model

Figure 2: Annual cycle of precipitation (mm day^{-1}) averaged over region (65^0E-88^0E, 18^0N-28^0N) as simulated by GFDL-HIRAM-C180 model, GFDL-HIRAM-C360 model, GFDL-CM3 model and GPCP observation.

Figure 3: Power spectrum of OLR (W m^{-2}) anomalies for June-September season of 30 years (1979-2008) averaged over region (65^0E-88^0E; 10^0N-28^0N) (a) observed (NOAA) (b) GFDL-HIRAM-C180 model (c) GFDL-HIRAM-C360 model (d) GFDL-CM3 model. Similarly for area averaged over Indian ocean region (75^0E-100^0E; 10^0S-5^0N) (e) observed (NOAA) (f) GFDL-HIRAM-C180 model (g) GFDL-HIRAM-C360 model (h) GFDL-CM3 model.

Figure 4: Same as in Figure 3 except averaged over Bay of Bengal (80^0E-100^0E;10^0N-20^0N) (a)observed (NOAA) (b)GFDL-HIRAM-C180 model (c) GFDL-HIRAM-C360 model (d) GFDL-CM3 model. Similarly for area averaged over West Pacific ocean (115^0E-140^0E;10^0N-25^0N) (e)observed (NOAA) (f)GFDL-HIRAM-C180 model (g) GFDL-HIRAM-C360 model (h) GFDL-CM3 model.

Figure 5: Variance of daily anomalies of zonal wind at 850hPa (m sec^{-1}) (contours) and the percent variance accounted for by intraseasonal 10-20 day bandpass filtered variance (shaded) of zonal wind at 850hPa for June-September of 30 years (1979-2008) (a)observed (NCEP/NCAR reanalysis) (b)GFDL-HIRAM-C180 model (c)GFDL-HIRAM-C360 model (d)GFDL-CM3 model. Similarly for OLR (e) observed (NOAA) (f) GFDL-HIRAM-C180 model (g) GFDL-HIRAM-C360 model (h) GFDL-CM3 model

Figure 6: June-September season lag-longitude plot of 5^0N-15^0N averaged 10-20 day filtered precipitation anomalies (shade) and 10-20 day filtered zonal wind at 850hPa anomalies (contours) regressed with a reference times series of 10-20 day filtered precipitation area averaged over south Bay of Bengal region (80^0E-90^0E; 5^0N-10^0N) for lag of day -25 to +25 (a) observed (precipitation : GPCP and 850hPa wind: NCEP-NCAR reanalysis) (b) GFDL-HIRAM-C180 model (c) GFDL- HIRAM-C360 model (d) GFDL-CM3 model. Similarly lag-latitude plot averaged over 80^0-100^0E (e) observed (precipitation: GPCP and 850hPa wind: NCEP/NCAR reanalysis) (f) GFDL-HIRAM-C180 model (g) GFDL- HIRAM-C360 model (h) GFDL-CM3 model.

Figure 1

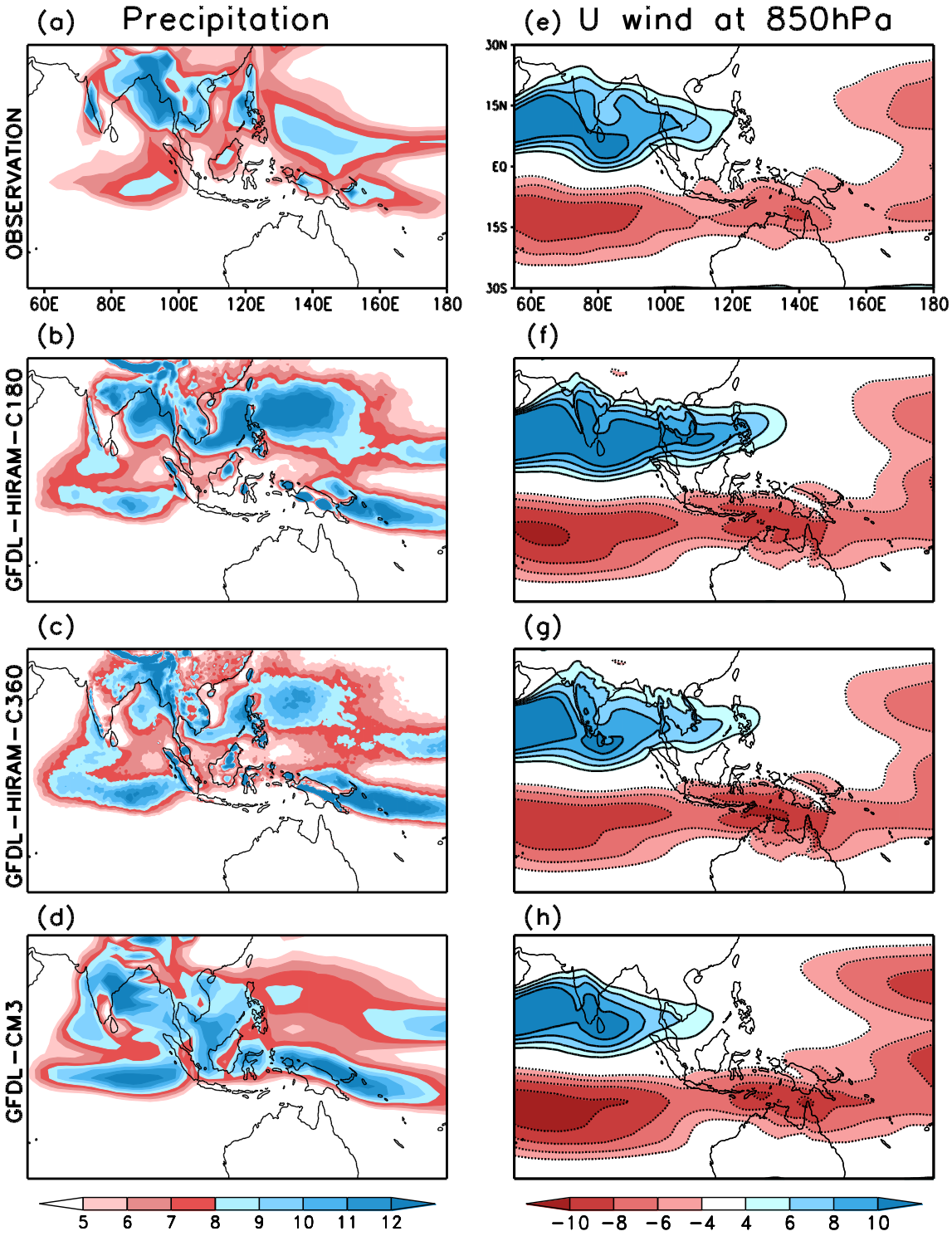
(a) Precipitation
(e) U wind at 850hPa
OBSERVATION
GFDL−HIRAM−C180
GFDL−HIRAM−C360
GFDL−CM3
(b)
(c)
(d)
(f)
(g)
(h)
30N
15N
EQ
15S
30S
60E
80E
100E
120E
140E
160E
180
5 6 7 8 9 10 11 12
−10 −8 −6 −4 4 6 8 10

Figure 2

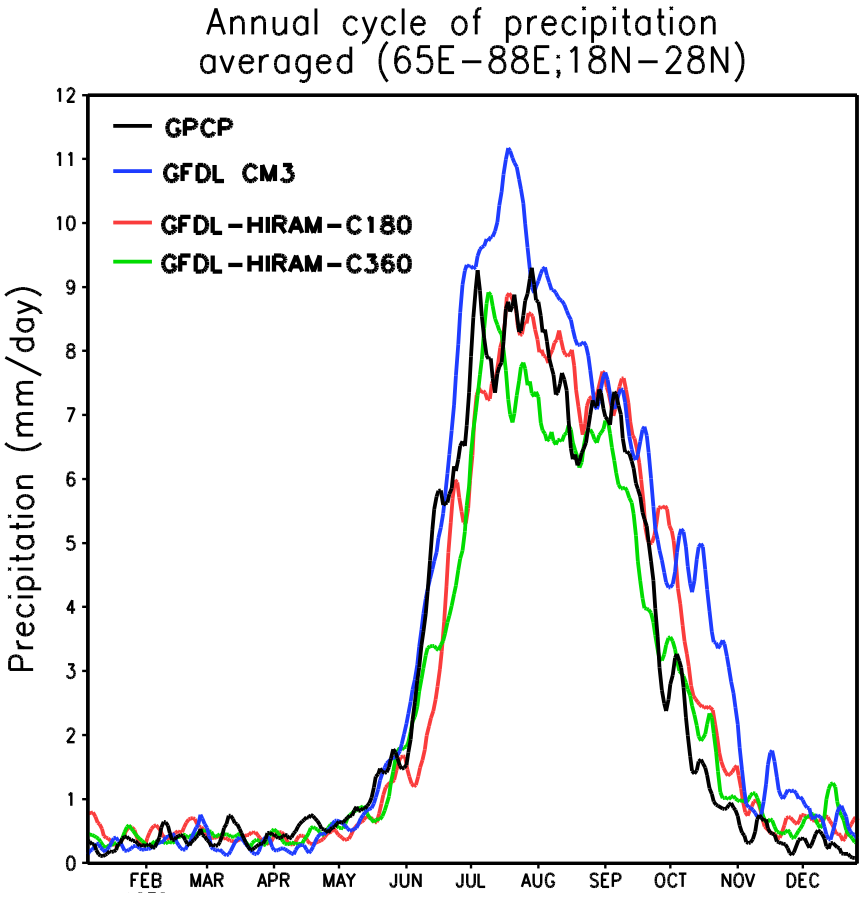
Annual cycle of precipitation
averaged (65E–88E;18N–28N)
GPCP
GFDL CM3
GFDL–HIRAM–C180
GFDL–HIRAM–C360
Precipitation (mm/day)
0
1
2
3
4
5
6
7
8
9
10
11
12
FEB
MAR
APR
MAY
JUN
JUL
AUG
SEP
OCT
NOV
DEC

Figure 3

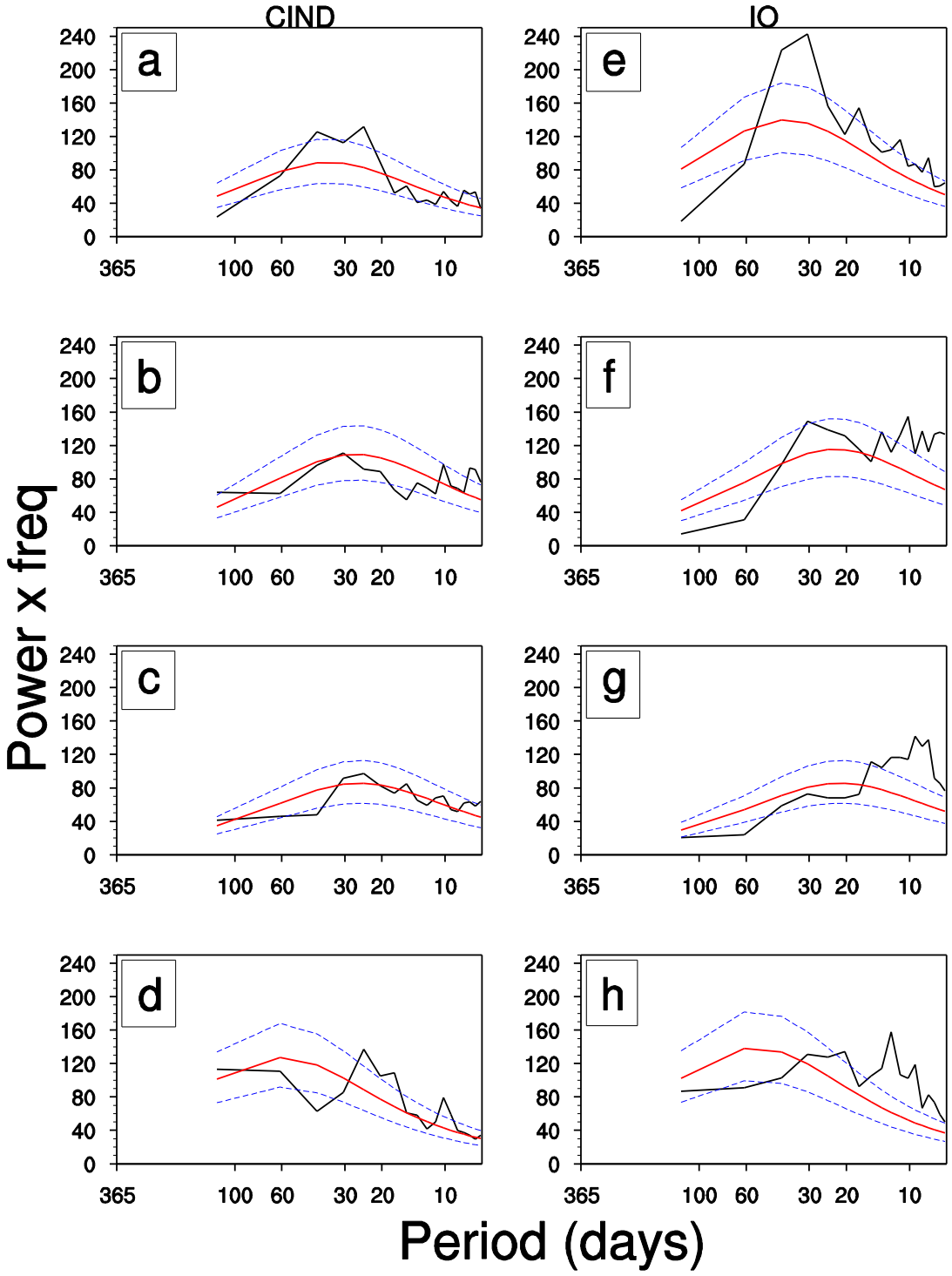
CIND
IO
a
b
c
d
e
f
g
h
240
200
160
120
80
40
0
365
100
60
30
20
10
Power x freq
Period (days)

Figure 4

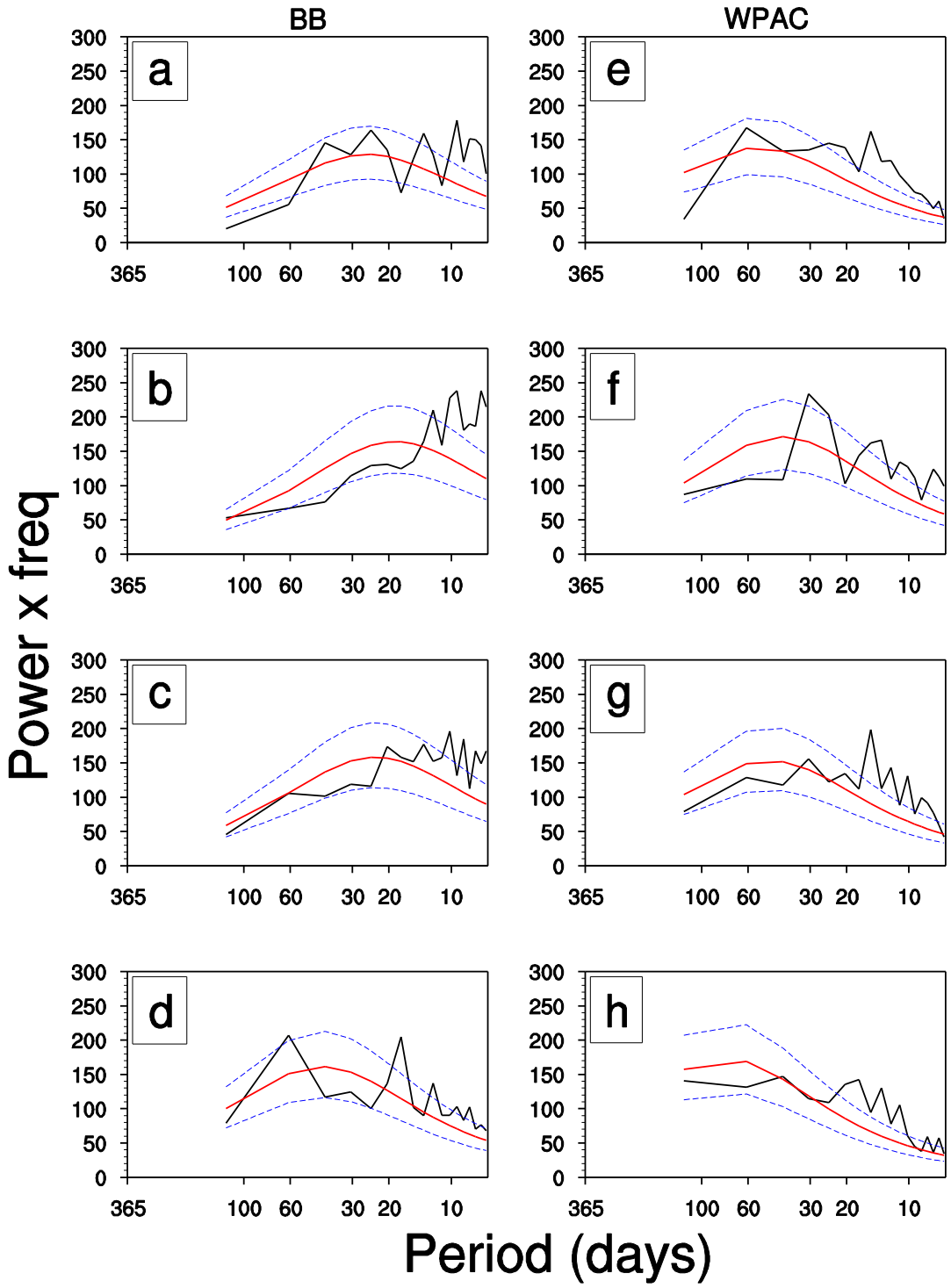
BB
WPAC
a
b
c
d
e
f
g
h
300
250
200
150
100
50
0
365
100
60
30
20
10
Power x freq
Period (days)

Figure 5

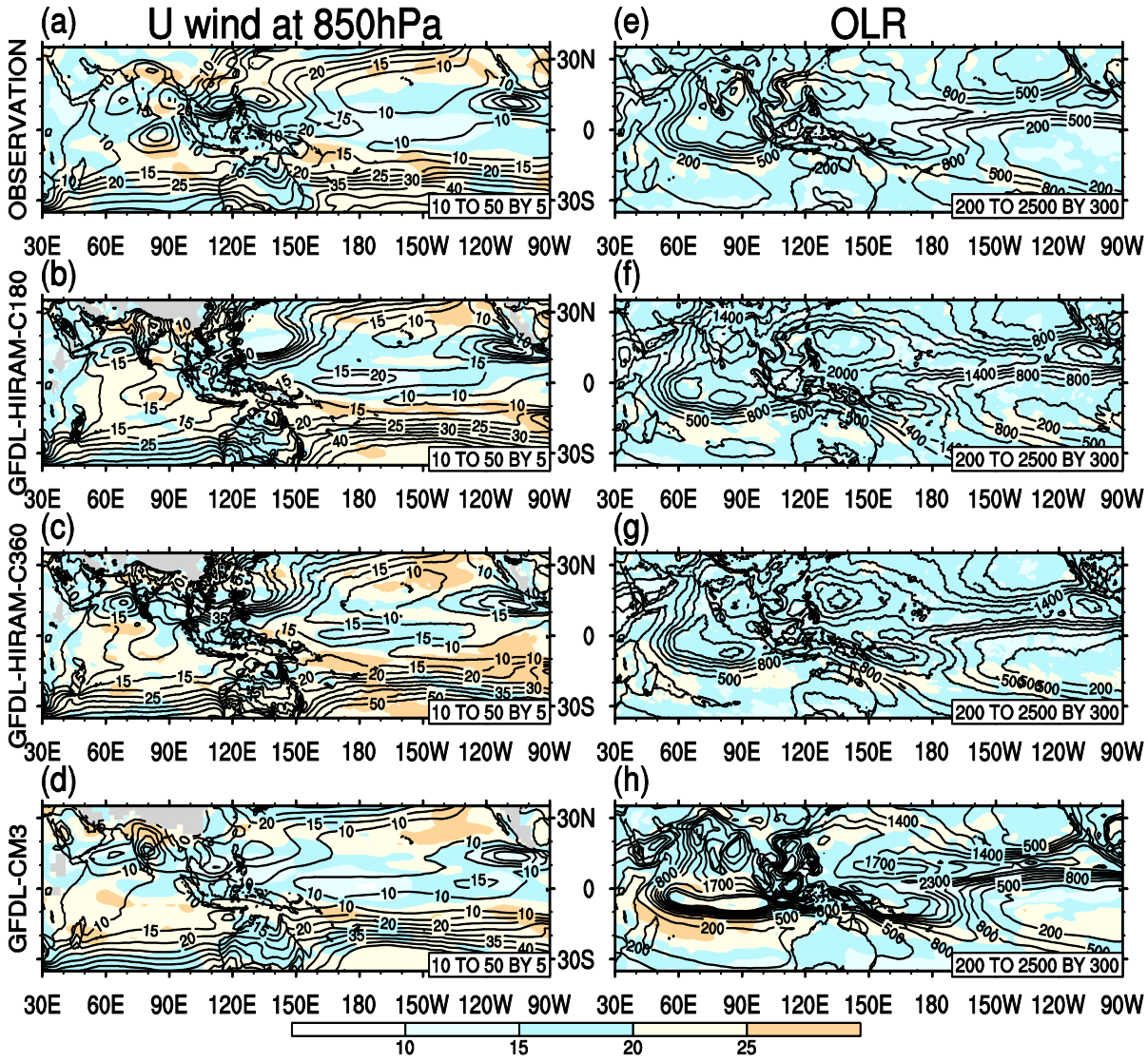
(a) U wind at 850hPa
(e) OLR
OBSERVATION
GFDL-HIRAM-C180
GFDL-HIRAM-C360
GFDL-CM3
(b)
(c)
(d)
(f)
(g)
(h)
10 TO 50 BY 5
200 TO 2500 BY 300
30N
0
30S
30E 60E 90E 120E 150E 180 150W 120W 90W
10 15 20 25

Figure 6

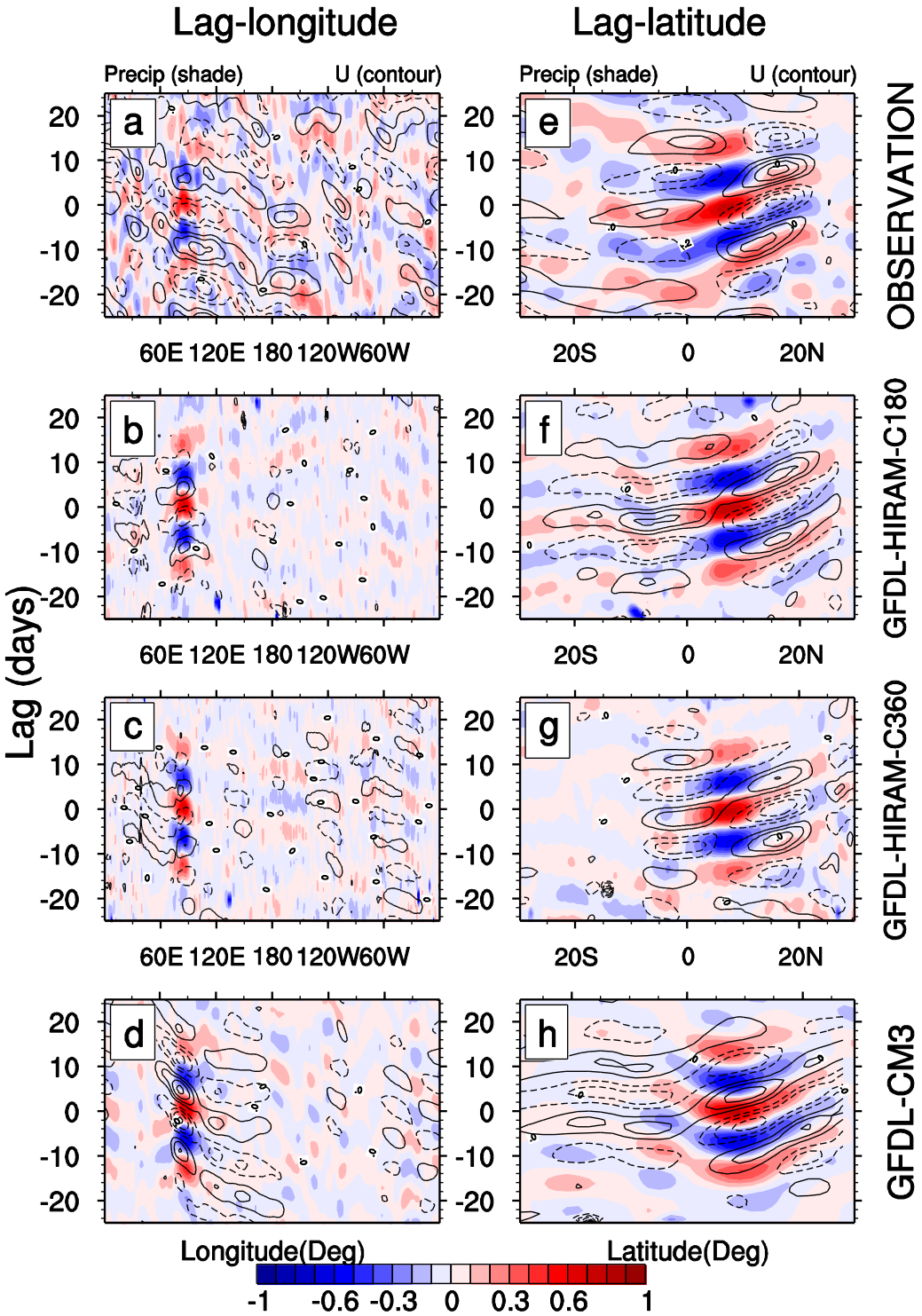
Lag-longitude
Lag-latitude
Precip (shade)
U (contour)
Precip (shade)
U (contour)
a
e
b
f
c
g
d
h
OBSERVATION
GFDL-HIRAM-C180
GFDL-HIRAM-C360
GFDL-CM3
Lag (days)
20
10
0
-10
-20
60E 120E 180 120W60W
20S
0
20N
Longitude(Deg)
Latitude(Deg)
-1
-0.6
-0.3
0
0.3
0.6
1